2080 nm long-wavelength, high-power dissipative soliton resonance in a dumbbell-shaped thulium-doped fiber laser

Hua Wang (王 华)[1,†], Tuanjie Du (杜团结)[2,†], Yanhong Li (李燕红)[2], Jinhai Zou (邹金海)[2], Kaijie Wang (王凯杰)[2], Fuyong Zheng (郑富永)[1], Junfeng Fu (付俊峰)[1], Jihai Yang (杨济海)[1], Hongyan Fu (付宏燕)[2], and Zhengqian Luo (罗正钱)[2,*]

[1]*Information and Communication Branch, State Grid Jiangxi Electric Power Corporation Ltd., Nanchang 330077, China*
[2]*Department of Electronic Engineering, Xiamen University, Xiamen 361005, China*
**Corresponding author: zqluo@xmu.edu.cn*

Received October 24, 2018; accepted December 20, 2018; posted online February 28, 2019

We demonstrate a 2080 nm long-wavelength mode-locked thulium (Tm)-doped fiber laser operating in the dissipative soliton resonance (DSR) regime. The compact all-fiber dumbbell-shaped laser is simply constructed by a 50/50 fiber loop mirror (FLM), a 10/90 FLM, and a piece of large-gain Tm-doped double-clad fiber pumped by a 793 nm laser diode. The 10/90 FLM is not only used as an output mirror, but also acts as a periodical saturable absorber for initiating DSR mode locking. The stable DSR pulses are generated at the center wavelength as long as 2080.4 nm, and the pulse duration can be tunable from 780 to 3240 ps as the pump power is increased. The maximum average output power is 1.27 W, corresponding to a pulse energy of 290 nJ and a nearly constant peak power of 93 W. This is, to the best of our knowledge, the longest wavelength for DSR operation in a mode-locked fiber laser.

OCIS codes: 060.3510, 140.4050, 140.3410.
doi: 10.3788/COL201917.030602.

Mode-locked (ML) Tm-doped fiber lasers (TDFLs) operating in the eye-safe spectral region of 2 μm[1–6] have attracted intense research interests due to their advantages for medicine[7], mid-infrared generation[8], material processing[9], gas sensing[10], and so on. At present, ML-TDFLs have been widely reported using a semiconductor saturable absorber mirror[11], carbon nanotubes[12], and two-dimensional materials[13–16]. However, the pulse energy obtained by these techniques is typically limited to 0.1–10 nJ[17]. Fortunately, dissipative soliton resonance (DSR) was theoretically predicted by Chang *et al.* and Akhmediev *et al.* in an ML fiber laser by solving the complex cubic–quintic Ginzburg–Landau equation[18,19], enabling an almost infinite boost of pulse energy without wave breaking[20,21]. They further predicted that DSR operation can be obtained in both normal and anomalous-dispersion regions[22,23], implying that large-energy DSR pulses could be obtained at any desired wavelength.

In 2009, Wu *et al.* observed the DSR operation for the first time, to the best of our knowledge, in a 1.56 μm normal-dispersion Er-doped ML fiber laser by the nonlinear polarization rotation technique[24]. Li *et al.* further obtained the DSR operation in an anomalous-dispersion ring fiber laser with a pulse energy of 79.5 nJ and a pulse width of 155 ns[25]. The ultra-wide tunable square-wave pulses in an Er-doped ML fiber laser were reported in 2012[26]. Subsequently, some research groups have reported DSR operation of ML fiber lasers based on the nonlinear optical loop mirror (NOLM) or nonlinear amplifying loop mirror (NALM) technique in a linear figure-eight or figure-nine cavity. Wang *et al.* successfully demonstrated the generation of DSR pulses in a figure-eight Er-doped fiber laser with a rectangular pulse width of 73.7 ns and pulse energy of 3.25 nJ[27]. In 2016, Krzempek *et al.* realized microjoule-level DSR pulse generation from a figure-nine Er:Yb double-clad fiber laser[28]. Semaan *et al.* further increased the DSR pulse energy to as high as 10 μJ in a figure-eight double-clad Er:Yb co-doped fiber laser[29]. Our research group proposed a short-length NOLM to significantly boost the peak power of the DSR pulse and realized the generation of 200 W peak power in a figure-nine Yb-doped fiber laser and 700 W peak power in a dumbbell-shaped Er:Yb co-doped fiber laser[30,31], respectively. It should be noted that most of these reports focused on 1 and 1.5 μm, but few works have been done in 2 μm wavelength DSR operation.

In 2015, Xu *et al.* reported the generation of DSR pulses in a 2 μm all-fiber TDFL with a 19.51 nJ pulse energy and a 6.19 ns pulse width[32]. Most recently, they demonstrated 1.96 μm DSR with a tunable pulse width from 3.74 to 72.19 ns and a peak power of 0.56 W, and two-stage amplifiers were used to increase the power and pulse energy[33]. Kharitonov *et al.* achieved a 2 μm figure-nine DSR ML fiber laser with an average output power of 670 mW, pulse energy of 400 nJ, and peak power of 7 W[34]. Recently, our group has demonstrated a 2 μm all-fiber compact σ-shaped DSR ML fiber laser, which delivered an average output power of 1.4 W, a maximum pulse energy of 353 nJ, and a maximum peak power of 84 W[35]. However, all of the previously reported DSR fiber lasers[30–38] are operating around 2 μm, and there is still strong motivation to extend longer wavelength DSR pulses directly from an ML fiber laser.

In this Letter, in order to obtain long-wavelength DSR pulses beyond 2 μm, we designed an all-fiber compact

dumbbell-shaped TDFL based on the NOLM technique. The laser can stably emit DSR pulses with the center wavelength of 2080.4 nm, a maximum average output power of 1.27 W, a maximum pulse energy of 290 nJ, and a peak power of 93 W. These are, to the best of our knowledge, the longest wavelength DSR pulses in an ML fiber laser.

Our experimental setup is shown in Fig. 1. The laser cavity simply consists of a 10 m double-clad Tm-doped fiber (TDF), a 793 nm laser diode (LD) together with a 793/2000 nm combiner and two fiber loop mirrors (FLMs). The TDF (Coractive, DCF-TM-6/128) as a high-gain medium has an absorption coefficient of ~1.5 dB/m at 790 nm and a group-velocity dispersion $\beta_2 = -81$ ps^2/km around 2000 nm. The two FLMs are used as the cavity mirrors to form the laser cavity. FLM1 is made of a 50/50 optical coupler (OC) as a highly reflective mirror, and FLM2 is constructed by a 10/90 OC, 11 m SM-1950 fiber, and an in-line fiber polarization controller (PC). The in-line PC in FLM2 is used to optimize the mode-locking operation. The reflectivity R of FLM2 is calculated to be ~36%, which can extract ~64% of the intra-cavity power[39]. FLM2 is not only used as an output mirror, but also acts as a periodic saturable absorber for initiating high-peak-power DSR. The modulation depth is ~36%, and the saturation power is about 94 W, which can be favorable in initiating self-started mode-locking at a low-pump-power level[39]. The cavity round-trip length is about 47 m for a fiber loop length L of 11 m, and the net cavity dispersion is about −3.78 ps^2.

The output optical spectrum is measured by a 1.3–5 μm laser spectrum analyzer (721B, Bristol Inc.). The characteristics of the DSR pulse trains and radio frequency (RF) spectrum are recorded by a 12.5 GHz photo-detector (ET-5000F, Electro-Optics Technology, Inc.) together with a 20 GS/s high-speed digital storage oscilloscope (Agilent Infiniium DSO9404A) or an RF spectrum analyzer. The output power is recorded by an optical power meter (Coherent, Field MaxII-TO).

In our experiment, the continuous-wave (CW) lasing threshold of the TDF laser was about 1.14 W. The self-starting ML state was observed when the pump power was increased over 2.5 W. The characteristics of the ML spectrum were summarized in Fig. 2. As seen in Fig. 2(a), the spectra were recorded under different pump powers of 2.63, 3.20, 4.35, and 5.49 W. The center wavelength of the ML laser did not move, and the spectral width never changed during the test. The optical spectra

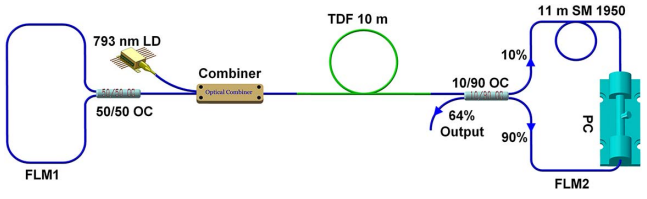

Fig. 1. Schematic of the compact dumbbell-shaped ML-TDFL.

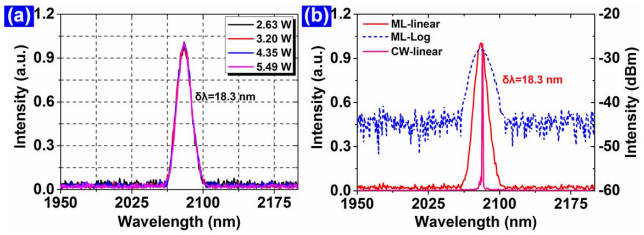

Fig. 2. (a) Optical spectral evolution under the pump powers of 2.63, 3.20, 4.35, and 5.49 W. (b) Optical spectra of both mode locking and CW at the pump power of 5.49 W.

of the mode locking maintained a Gaussian profile, while the pump power increased. As shown in Fig. 2(b), the CW lasing at 2082.1 nm has a narrow linewidth of 1.1 nm. Compared with the CW optical spectrum, the ML spectrum is significantly broadened, while the pump power is over 2.5 W and has a 3 dB bandwidth of 18.3 nm. The long-wavelength oscillation in the laser cavity could be mainly attributed to the uses of the long-length double-clad TDF and low cavity loss.

In order to further investigate the output characteristics of the DSR operation, we recorded the evolution of the DSR pulse, as seen in Figs. 3(a) and 3(b). The DSR pulse duration monotonously increased from 0.78 to 3.24 ns, and the pulse profile maintained a rectangular shape when the pump power gradually increased from 2.29 to 7.75 W. The optical spectral and pulse evolutions are in good agreement with features of the DSR operation reported previously[16–38]. The calculated time-bandwidth product is in the range of 989.4–4109.8. This indicates that the pulse is largely chirped, which is a typical feature of DSR. Moreover, it has been reported that the compression of the DSR pulse is very difficult, because the DSR pulse exhibits a unique chirp feature: a low chirp across the center regime and large linear chirps at both pulse edges[40]. In our experiment, we tried to compress it by

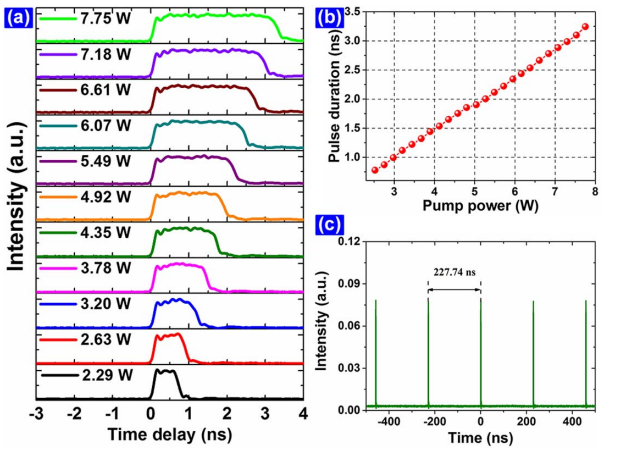

Fig. 3. Output time-domain characteristics. (a) Single pulse envelopes with different pump powers. (b) The pulse duration as a function of the pump power. (c) Typical pulse trains at the pump power of 5.49 W.

a piece of dispersion compensation fiber, but we failed. Figure 3(c) shows typical pulse trains at the pump power of 5.49 W, where the pulse-to-pulse interval is 227.74 ns, corresponding to the cavity round-trip time.

Figure 4 shows the characteristic of the DSR operation in the frequency domain. As given in Fig. 4(a), the wide-span RF spectra up to 500 MHz were recorded under different pump powers of 4.35, 5.49, 6.61, and 7.75 W. Interestingly, there is a modulation frequency period in each widespan RF spectrum, which corresponds to the pulse duration in the temporal domain by Fourier transformation. To further demonstrate the characteristics of the DSR pulses in the RF domain, the RF spectrum up to 100 MHz and the typical RF spectrum around the fundamental frequency are plotted in Figs. 4(b) and 4(c). The fundamental frequency peak is locked at the cavity repetition rate of 4.3652 MHz by using a 10 Hz resolution bandwidth. The RF signal-to-noise ratio (SNR) is about ~57 dB, indicating CW mode-locking operation.

We also recorded the average output power, pulse energy, and peak power as functions of the pump power. As seen in Fig. 5, the average output power and pulse energy linearly increased with the pump power. The maximum average output power is about 1.27 W without any saturation, and the maximum pulse energy is about 290 nJ at a pump power of 7.75 W, respectively. Due to the peak power clamping effect induced by the periodic saturable absorption of the 10/90 FLM, the peak power is clamped at a nearly constant value of 93 W.

In conclusion, we have demonstrated a long-wavelength, high-power, dumbbell-shaped ML-TDFL operating in the DSR regime. A 10/90 FLM as the output mirror provided the periodic saturable absorber that played a key role in realizing mode locking. Self-started mode-locking at 2080.4 nm stably generated rectangular DSR pulses with pulse duration tunable from 0.78 to 3.24 ns and a

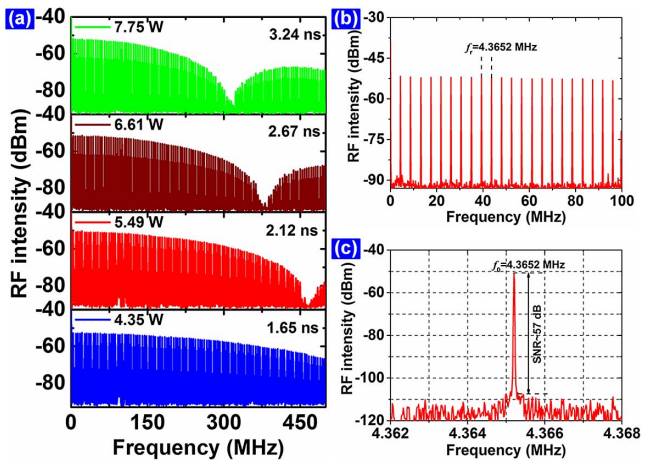

Fig. 4. Output frequency domain characteristics. (a) The RF spectra evolution as a function of pump power. (b) The widespan RF spectrum up to 100 MHz at the pump power of 5.49 W. (c) RF output spectrum at the fundamental frequency at the pump power of 5.49 W.

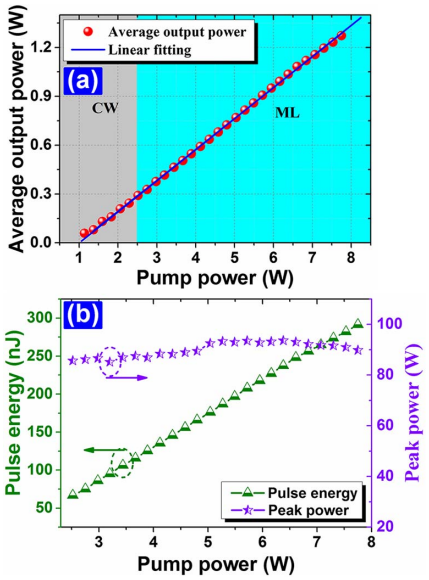

Fig. 5. (a) Average output power as a function of pump power. (b) Peak power and pulse energy as functions of pump power.

4.3652 MHz repetition rate. The DSR pulses have a maximum average output power of 1.27 W, a pulse energy of 290 nJ, and a nearly constant peak power of 93 W.

This work was supported in part by the Research Fund of State Grid Corporation of China (No. 52183516000B), the National Natural Science Foundation of China (No. 61475129), the Natural Science Foundation of Fujian Province (No. 2017J06016), and the Fundamental Research Funds for the Central Universities (No. 20720180057).

†These authors contributed equally to this work.

References

1. S. D. Jackson and T. A. King, J. Lightwave Technol. **17**, 948 (1999).
2. M. Zhang, E. J. R. Kelleher, T. H. Runcorn, V. M. Mashinsky, O. I. Medvedkov, E. M. Dianov, Z. Sun, D. Popa, T. Hasan, A. C. Ferrari, B. H. Chapman, S. V. Popov, and J. R. Taylor, in *CLEO: 2013, OSA Technical Digest* (online) (2013), paper CW1M.5.
3. K. Kieu and F. W. Wise, IEEE Photon. Technol. Lett. **21**, 128 (2009).
4. F. Haxsen, A. Ruehl, M. Engelbrecht, D. Wandt, U. Morgner, and D. Kracht, Opt. Express **16**, 20471 (2008).
5. B. Ibarra-Escamilla, M. Durán-Sánchez, R. I. Álvarez-Tamayo, B. Posada-Ramírez, P. Prieto-Cortés, E. A. Kuzin, J. L. Cruz, and M. V. Andrés, J. Opt. **20**, 085702 (2018).
6. M. Durán-Sánchez, R. I. Álvarez-Tamayo, B. Posada-Ramírez, B. Ibarra-Escamilla, E. A. Kuzin, J. L. Cruz, and M. V. Andrés, IEEE Photon. Technol. Lett. **29**, 1820 (2017).
7. N. M. Fried and K. E. Murray, J. Endourol. **19**, 25 (2005).
8. J. Luo, B. Sun, J. Ji, E. L. Tan, Y. Zhang, and X. Yu, Opt. Lett. **42**, 1568 (2017).
9. G. Genty, J. M. Dudley, and B. J. Eggleton, Appl. Phys. B **94**, 187 (2008).
10. K. Bremer, A. Pal, S. Yao, E. Lewis, R. Sen, T. Sun, and K. T. V. Grattan, Appl. Opt. **52**, 3957 (2013).
11. J. Li, D. D. Hudson, Y. Liu, and S. D. Jackson, Opt. Lett. **37**, 3747 (2012).

12. Y. Meng, Y. Li, Y. Xu, and F. Wang, Sci. Rep. **7**, 45109 (2017).
13. M. Zhang, E. J. R. Kelleher, F. Torrisi, Z. Sun, T. Hasan, D. Popa, F. Wang, A. C. Ferrari, S. V. Popov, and J. R. Taylor, Opt. Express **20**, 25077 (2012).
14. Z. Sun, T. Hasan, F. Torrisi, D. Popa, G. Privitera, F. Wang, F. Bonaccorso, D. M. Basko, and A. C. Ferrari, ACS Nano **4**, 803 (2010).
15. M. Pawliszewska, Y. Ge, Z. Li, H. Zhang, and J. Sotor, Opt. Express **25**, 16916 (2017).
16. B. Guo, Chin. Opt. Lett. **16**, 020004 (2018).
17. H. Zhang, D. Tang, R. J. Knize, L. Zhao, Q. Bao, and K. P. Loh, Appl. Phys. Lett. **96**, 111112 (2010).
18. N. Akhmediev, J. M. Soto-Crespo, and P. Grelu, Phys. Lett. A **372**, 3124 (2008).
19. W. Chang, A. Ankiewicz, J. M. Soto-Crespo, and N. Akhmediev, Phys. Rev. A **78**, 023830 (2008).
20. L. Liu, J. H. Liao, Q. Y. Ning, W. Yu, A. P. Luo, S. H. Xu, Z. C. Luo, Z. M. Yang, and W. C. Xu, Opt. Express **21**, 27087 (2013).
21. D. Li, D. Tang, L. Zhao, and D. Shen, J. Lightwave Technol. **33**, 3781 (2015).
22. W. Chang, J. M. Soto-Crespo, A. Ankiewicz, and N. Akhmediev, Phys. Rev. A **79**, 033840 (2009).
23. W. Chang, A. Ankiewicz, J. M. Soto-Crespo, and N. Akhmediev, J. Opt. Soc. Am. B **25**, 1972 (2008).
24. X. Wu, D. Y. Tang, H. Zhang, and L. M. Zhao, Opt. Express **17**, 5580 (2009).
25. X. Li, X. Liu, X. Hu, L. Wang, H. Lu, Y. Wang, and W. Zhao, Opt. Lett. **35**, 3249 (2010).
26. X. Zhang, C. Gu, G. Chen, B. Sun, L. Xu, A. Wang, and H. Ming, Opt. Lett. **37**, 1334 (2012).
27. S. K. Wang, Q. Y. Ning, A. P. Luo, Z. B. Lin, Z. C. Luo, and W. C. Xu, Opt. Express **21**, 2402 (2013).
28. K. Krzempek, J. Sotor, and K. Abramski, Opt. Lett. **41**, 4995 (2016).
29. G. Semaan, F. B. Braham, J. Fourmont, M. Salhi, F. Bahloul, and F. Sanchez, Opt. Lett. **41**, 4767 (2016).
30. Y. Huang, Z. Luo, F. Xiong, Y. Li, M. Zhong, Z. Cai, H. Xu, and H. Fu, Opt. Lett. **40**, 1097 (2015).
31. T. Du, Z. Luo, R. Yang, Y. Huang, Q. Ruan, Z. Cai, and H. Xu, Opt. Lett. **42**, 462 (2017).
32. Y. Xu, Y. L. Song, G. G. Du, P. G. Yan, C. Y. Guo, G. L. Zheng, and S. C. Ruan, IEEE Photon. J. **7**, 1502007 (2015).
33. J. Zhao, D. Ouyang, Z. Zheng, M. Liu, X. Ren, C. Li, S. Ruan, and W. Xie, Opt. Express **24**, 12072 (2016).
34. S. Kharitonov and C. S. Brès, in *Conference on Lasers and Electro-Optics Europe & European Quantum Electronics Conference (CLEO/Europe-EQEC)* (2017), paper CJ-13-4.
35. T. Du, W. Li, Q. Ruan, K. Wang, N. Chen, and Z. Luo, Appl. Phys. Express **11**, 052701 (2018).
36. T. Wang, W. Ma, Q. Jia, Q. Su, P. Liu, and P. Zhang, IEEE J. Sel. Top. Quantum Electron. **23**, 1102011 (2018).
37. B. Ibarra-Escamilla, M. Durán-Sánchez, B. Posada-Ramírez, H. Santiago-Hernández, R. I. Álvarez-Tamayo, D. S. Llave, M. Bello-Jiménez, and E. A. Kuzin, IEEE Photon. J. **10**, 1503907 (2018).
38. W. Ma, T. Wang, Q. Su, F. Wang, J. Zhang, C. Wang, and H. Jiang, Opt. Express **26**, 12514 (2018).
39. N. J. Doran and D. Wood, Opt. Lett. **13**, 56 (1988).
40. D. Li, L. Li, J. Zhou, L. Zhao, D. Tang, and D. Shen, Sci. Rep. **6**, 23631 (2016).